Ultra-Fast Perpendicular Spin–Orbit Torque MRAM

Murat Cubukcu, Olivier Boulle, Nikolai Mikuszeit, Claire Hamelin, Thomas Bracher, Nathalie Lamard, Marie-Claire Cyrille, Liliana D. Buda-Prejbeanu, Kévin Garello, Ioan Mihai Miron, et al.

Ultra-fast perpendicular Spin Orbit Torque MRAM

Murat Cubukcu*,[1], Olivier Boulle[1, †], Nikolaï Mikuszeit[1], Claire Hamelin[1], Thomas Brächer[1],

Nathalie Lamard[6], Marie-Claire Cyrille[6] , Liliana Buda-Prejbeanu[1], Kevin Garello[2], Ioan

Mihai Miron[1], O. Klein[1], G. de Loubens[4], V. V. Naletov[1,4,5], Juergen Langer[3], Berthold

Ocker[3], Pietro Gambardella[2] and Gilles Gaudin[1]

1 Univ. Grenoble Alpes, CEA, CNRS, Grenoble INP, INAC, SPINTEC, F-38000 Grenoble, France

[2] Department of Materials, ETH Zurich, Hönggerbergring 64, CH-8093 Zürich, Switzerland

[3] Singulus Technologies, Hanauer Landstr, 103, 63796, Kahl am Main, Germany

[4] Service de Physique de l'Etat Condensé (CNRS URA 2464), CEA Saclay, 91191 Gif-sur-Yvette,

France

 [5] Institute of Physics, Kazan Federal University, Kazan 420008, Russian Federation

[6] CEA Leti, F-38000 , Grenoble, France

We demonstrate ultra-fast (down to 400 ps)   bipolar magnetization switching of a three-terminal perpendicular Ta/FeCoB/MgO/FeCoB magnetic tunnel junction. The critical current density rises significantly as the current pulse shortens below 10 ns, which translates into a minimum in the write energy in the ns range. Our results show that SOT-MRAM allows fast

1

and low-power write operations, which renders it promising for non-volatile cache memory applications.

The introduction of non-volatility at the cache level is a major challenge to the IT industry as it would lead to a large decrease of the power consumption of microprocessors by minimizing their static and dynamic power consumption and pave the way towards normally-off/instant-on computing. Among other technologies, STT-MRAM has been identified as a promising candidate for the non-volatile replacement of SRAM cache memory technology[1]. STT-MRAM combines CMOS compatibility, high retention time (10 years), large endurance and relatively fast write time (down to 4 ns for reliable switching in perpendicular STT-MRAM[2]). However, cache memory applications typically require faster operations (~ns for L1 cache) combined with a large endurance due to their high access rate. Very fast switching (sub-ns) has been recently demonstrated using stacks where the magnetizations of the free and the fixed layers are perpendicular[3]–[5]. However, this gain in operation speed comes at the expense of a rise in the current flowing through the tunnel barrier. As a consequence, manufacturers are currently facing reliability issues due to the accelerated aging of the tunnel barrier when injecting these high write current densities[6], [7]. Another drawback of STT-MRAM is that reading and writing use the same current path. This results in an undesired writing during the read-out of the bit[7] as well as a high read power since the tunnel barrier needs to have a very small resistance to sustain the large writing current densities.

Recently, we have proposed a novel memory concept, named Spin-Orbit Torque-MRAM (SOT-MRAM), that combines the STT advantages and naturally solves the above mentioned issues[8]–[10]. The memory is based on the discovery that a current flowing in the plane of a magnetic multilayer with structural inversion asymmetry, such as $Pt/Co/AlO_x$, exerts a torque on the magnetization, which can lead to magnetization reversal[9], [11], [12]. Such a torque

3

arises from the conversion of the orbital to spin angular momentum through the spin Hall effect in the heavy metal and/or the Rashba-Edelstein effect at the interfaces[9], [13]–[15]. The key advantage of the SOT-MRAM is that writing and reading are decoupled due to their independent current paths. Thus, the SOT-MRAM intrinsically solves the reliability issues in current STT-MRAM promising a potentially unlimited endurance.

To be a strong candidate for non-volatile cache memory applications, SOT-MRAM needs to be fast. We recently demonstrated deterministic switching induced by current pulses shorter than 200 ps in dots made of Pt/Co/AlOx stacks[12]. However, the use of a Pt seed layer in MgO based MTJ does not allow to reach the high TMR ratio needed for memory applications[16], [17] (>100%), as it promotes a (111) fcc texture while a (100) bcc structure at the CoFe/MgO interface is needed to achieve high TMR [18]–[20]On the contrary, the Ta/FeCoB/MgO/FeCoB MTJ stacks commonly used for STT-MRAM seem ideal for SOT-MRAM since they combine a high TMR, a perpendicular magnetization[21] and a large spin Hall effect in Ta[22]. In this article, we demonstrate that magnetization switching can be achieved by very short current pulses (down to 400 ps) in Ta/FeCoB/MgO three-terminal SOT-MRAM memory cells. Our results show that SOT-MRAM allows for fast, and low-power write operations, rendering it promising for non-volatile cache memory applications.

The magnetic tunnel junctions (MTJ) was deposited by magnetron sputtering using a Singulus Timaris® deposition machine with the following structure[23]–[25] 10 Ta/1 $Fe_{60}Co_{20}B_{20}$/MgO/ 1.3 $Fe_{60}Co_{20}B_{20}$/0.3 Ta/FM_1/Ru0.85/FM_2 (thicknesses in nm), where FM_1=[0.4 Co/ 0.4 Cu/ 1.4 Pt]$_{x5}$ /0.6 Co and FM_2=0.6 Co/[0.4 Cu/ 1.4 Pt/ 0.4 Co]$_{x12}$/ 0.4 Cu/2 Pt (see Fig. 1(a)). Functional three-terminal single cells with lateral dimensions down to 150 nm diameter on top of a 330

4

nm wide Ta track were fabricated as described in Ref.[26]   The results presented here are obtained from a sample with a 275 nm diameter MTJ on top of a 635 nm Ta track (see Fig.1 (b)). All measurement are carried out at room temperature. Figure 1 (c) shows a typical TMR hysteresis cycle corresponding to the successive reversal of the FeCoB (1 nm) free layer and pinned layer, the magnetic field being applied perpendicularly to the sample plane. A TMR of up to 55%, associated with a sharp reversal of the magnetization of the free layer, is observed. The resistance area product of the junction is about 600 $\Omega.\mu m^2$. For the current induced magnetization switching experiments, current pulses are injected in the Ta bottom track using a fast voltage pulse generator whereas the TMR signal is measured using a DC voltage source connected to the MTJ in series with a 1MΩ resistor. This resistor prevents high voltages spikes on the MTJ during the pulse injection. A 100 Ω resistor was connected in parallel to the track to minimize the impedance mismatch. The pulse rise time is 220 ps for pulse widths τ_P <2 ns, and 1.5 ns for wider pulses. The pulse width is defined as the full width at half maximum.

Figure 2 (a) shows the TMR signal measured after the pulse injection as a function of the amplitude of the current pulse injected in the track. An in-plane magnetic field $\mu_0 H_{ip}$=100 mT is applied along the current direction to allow for the bipolar switching[9]. The current pulse is 550 ps long. Starting from the low resistance state and increasing the current, a sharp increase in the TMR signal is observed above a positive threshold pulse amplitude, demonstrating the reversal of the magnetization of the FeCoB bottom free layer from the parallel (P) to the anti-parallel (AP) configurations of the magnetizations. From the AP configuration, a large enough negative current allows to go back to the P configuration. This demonstrates the writing of a perpendicular SOT-MRAM memory cell by a 550 ps current pulse and its reading by the TMR signal. Note that the switching current for the P to AP

5

switching is slightly lower than the one for the AP to P, which can be explained by the dipolar interaction between the bottom free layer and the not fully compensated synthetic antiferromagnet. The corresponding switching-current density is about 3.3×10^{12} A/m². The switching probability from the P to the AP configuration as a function of the amplitude of the current for different pulse widths is plotted in Fig. 2(b) (each point is an average over 30 events) [27]. Interestingly, recent time-resolved X-ray microscopy imaging of the spin orbit torque driven magnetization reversal of Pt/Co/AlOx dots revealed that the switching probability measured electrically is not the probability of an on/off event, but more likely the fraction of the magnetic layer area that has switched[28]. The same measurements show that there are no ringing or after – pulse effects associated to switching.

Magnetization switching is observed in the whole range of pulse widths from 400 ps to 2.5 µs and is bipolar: positive currents lead to a magnetization switching from P to AP, whereas negative currents lead to a switching from AP to P. The switching current I_c strongly depends on the pulse length τ_P (see Fig. 3(a)). For $\tau_P > 10$ ns, J_c changes little with τ_P and scales approximately linearly on log(τ_P) suggesting a thermally activated regime where stochastic fluctuations help the magnetization to overcome the reversal energy barrier [29], [30]. For $\tau_P <$ 10 ns, a large increase of J_c is observed as τ_P decreases and J_c scales linearly on $1/\tau_P$ (see Fig.3(a) inset). For $\tau_P <$ 10 ns, a large increase of J_c is observed as τ_P decreases and J_c scales linearly on $1/\tau_P$ (see Fig.3(a) inset). This scaling is reminiscent of early spin transfer torque predictions [31] and experiments [32] where the injected spin current polarization is aligned along the uniaxial anisotropy axis. Such a scaling is expected from the conservation of spin angular momentum, assuming the magnetization is spatially homogeneous (macrospin approximation). A different scaling is however expected in our spin orbit torque geometry where the current spin

6

polarization is aligned perpendicular to the uniaxial anisotropy axis [12], [33]. On the other hand, several experimental study have shown that for lateral sizes typically larger than 50 nm, the magnetization reversal by spin transfer and spin orbit torques occurs by domain nucleation followed by domain wall propagation[28], [34]–[41]. In such a case, a $1/\tau_P$ scaling of the critical current is expected, which expresses that the switching time is the time for a nucleated domain wall to travel across the dot.

As expected, the switching current depends also on the external in-plane magnetic field H_{ip} and decreases as H_{ip} increases (Fig. 3(a)). The corresponding write energy E=RI²τ_P is plotted in Fig. 3(b) as function of τ_P, assuming it is dissipated in a 3 kΩ resistance standing for the Ta track and the addressing transistor. The energy depends non-monotonously on τ_P with a large increase of the energy as τ_P decreases for τ_P<1 ns. Interestingly, a minimum in the write energy is observed between 1 and 3 ns. This feature is explained by the crossover between the thermally activated regime for large pulse width and the short pulse width regime. The energy scale extrapolated for a 50 nm wide and 3 nm thick Ta track is shown in blue on the right vertical axis A write energy of about 95 fJ at 1.5 ns can be reached, associated with a write current of about 180 µA, which is similar to the best results obtained so far for current perpendicular STT-MRAM technology[42], [43].

In conclusion, we demonstrate ultra-fast (down to 400 ps) bipolar and deterministic writing of perpendicular three-terminal spin-orbit torque (SOT)-MRAM single cells with a Ta/CoFeB/MgO/CoFeB MTJ structure. The switching current density rises significantly as the pulse shortens below 10 ns. This translates into a write energy minimum in the ns range.

These experimental results extrapolate to a switching current of around 180 µA at 1.5 ns for 50 nm track width. This makes SOT-MRAM promising for a power efficient non-volatile cache

7

memory application.

* Current address : Cavendish laboratory, University of Cambridge, JJ Thomson Avenue, Cambridge, CB3 0HE UK,

† e-mail: olivier.boulle@cea.fr

References

[1] The International Technology Roadmap for Semiconductors, "http://www.itrs.net/Links/2013ITRS/2013Chapters/2013ERD.pdf."

[2] G. Jan *et al.*, "Demonstration of fully functional 8Mb perpendicular STT-MRAM chips with sub-5ns writing for non-volatile embedded memories," in *2014 Symposium on VLSI Technology (VLSI-Technology): Digest of Technical Papers*, 2014, pp. 1–2.

[3] H. Liu, D. Bedau, D. Backes, J. A. Katine, J. Langer, and A. D. Kent, "Ultrafast switching in magnetic tunnel junction based orthogonal spin transfer devices," *Appl. Phys. Lett.*, vol. 97, no. 24, p. 242510, 2010.

[4] M. M. de Castro *et al.*, "Precessional spin-transfer switching in a magnetic tunnel junction with a synthetic antiferromagnetic perpendicular polarizer," *J. Appl. Phys.*, vol. 111, no. 7, p. 07C912, Apr. 2012.

[5] G. E. Rowlands *et al.*, "Deep subnanosecond spin torque switching in magnetic tunnel junctions with combined in-plane and perpendicular polarizers," *Appl. Phys. Lett.*, vol. 98, no. 10, p. 102509, Mar. 2011.

[6] G. Panagopoulos, C. Augustine, and K. Roy, "Modeling of dielectric breakdown-induced time-dependent STT-MRAM performance degradation," in *Device Research Conference (DRC), 2011 69th Annual*, 2011, pp. 125–126.

[7] W. S. Zhao *et al.*, "Failure and reliability analysis of STT-MRAM," *Microelectron. Reliab.*, vol. 52, no. 9–10, pp. 1848–1852, Sep. 2012.

[8] G. Gaudin, I. M. Miron, P. Gambardella, and A. Schuhl, "A writable magnetic memory element," 12/899,072; 12/899,091; 12/959,980.

[9] I. M. Miron *et al.*, "Perpendicular switching of a single ferromagnetic layer induced by in-plane current injection," *Nature*, vol. 476, no. 7359, pp. 189–193, 2011.

[10] G. Prenat, K. Jabeur, G. D. Pendina, O. Boulle, and G. Gaudin, "Beyond STT-MRAM, Spin Orbit Torque RAM SOT-MRAM for High Speed and High Reliability Applications," in *Spintronics-based Computing*, W. Zhao and G. Prenat, Eds. Springer International Publishing, 2015, pp. 145–157.

[11] C. Onur Avci *et al.*, "Magnetization switching of an MgO/Co/Pt layer by in-plane current injection," *Appl. Phys. Lett.*, vol. 100, no. 21, p. 212404, May 2012.

[12] K. Garello *et al.*, "Ultrafast magnetization switching by spin-orbit torques," *Appl. Phys. Lett.*, vol. 105, no. 21, p. 212402, Nov. 2014.

[13] L. Liu, C.-F. Pai, Y. Li, H. W. Tseng, D. C. Ralph, and R. A. Buhrman, "Spin-Torque Switching with the Giant Spin Hall Effect of Tantalum," *Science*, vol. 336, no. 6081, pp. 555–558, May 2012.

[14] K. Garello *et al.*, "Symmetry and magnitude of spin-orbit torques in ferromagnetic heterostructures," *Nat. Nanotechnol.*, vol. 8, no. 8, pp. 587–593, Aug. 2013.

[15] J. Kim *et al.*, "Layer thickness dependence of the current-induced effective field vector in Ta|CoFeB|MgO," *Nat. Mater.*, 2012.

[16] Y. J. Song *et al.*, "Highly functional and reliable 8Mb STT-MRAM embedded in 28nm logic," in *2016 IEEE International Electron Devices Meeting (IEDM)*, 2016, p. 27.2.1-27.2.4.

[17] J. J. Kan *et al.*, "Systematic validation of 2x nm diameter perpendicular MTJ arrays and MgO barrier for sub-10 nm embedded STT-MRAM with practically unlimited endurance," in *2016 IEEE International Electron Devices Meeting (IEDM)*, 2016, p. 27.4.1-27.4.4.

[18] S. S. P. Parkin *et al.*, "Giant tunnelling magnetoresistance at room temperature with MgO (100) tunnel barriers," *Nat. Mater.*, vol. 3, no. 12, pp. 862–867, Dec. 2004.

[19] W. H. Butler, X.-G. Zhang, T. C. Schulthess, and J. M. MacLaren, "Spin-dependent tunneling conductance of $\mathrm{Fe}|\mathrm{MgO}|\mathrm{Fe}$ sandwiches," *Phys. Rev. B*, vol. 63, no. 5, p. 054416, Jan. 2001.

[20] S. Yuasa, T. Nagahama, A. Fukushima, Y. Suzuki, and K. Ando, "Giant room-temperature magnetoresistance in single-crystal Fe/MgO/Fe magnetic tunnel junctions," *Nat. Mater.*, vol. 3, no. 12, pp. 868–871, Dec. 2004.

[21] S. Ikeda *et al.*, "A perpendicular-anisotropy CoFeB–MgO magnetic tunnel junction," *Nat. Mater.*, vol. 9, no. 9, pp. 721–724, Sep. 2010.

[22] L. Liu, C.-F. Pai, Y. Li, H. W. Tseng, D. C. Ralph, and R. A. Buhrman, "Spin-Torque Switching with the Giant Spin Hall Effect of Tantalum," *Science*, vol. 336, no. 6081, pp. 555–558, May 2012.

[23] D. C. Worledge *et al.*, "Spin torque switching of perpendicular Ta|CoFeB|MgO-based magnetic tunnel junctions," *Appl. Phys. Lett.*, vol. 98, no. 2, p. 022501, 2011.

[24] L. Cuchet, B. Rodmacq, S. Auffret, R. C. Sousa, C. Ducruet, and B. Dieny, "Influence of a Ta spacer on the magnetic and transport properties of perpendicular magnetic tunnel junctions," *Appl. Phys. Lett.*, vol. 103, no. 5, p. 052402, 2013.

[25] L. Cuchet, B. Rodmacq, S. Auffret, R. C. Sousa, and B. Dieny, "Influence of magnetic electrodes thicknesses on the transport properties of magnetic tunnel junctions with perpendicular anisotropy," *Appl. Phys. Lett.*, vol. 105, no. 5, p. 052408, Aug. 2014.

[26] M. Cubukcu *et al.*, "Spin-orbit torque magnetization switching of a three-terminal perpendicular magnetic tunnel junction," *Appl. Phys. Lett.*, vol. 104, no. 4, p. 042406, Jan. 2014.

[27] "Higher current density/pulse width could not been probed due to the limited life time of the measured samples, which was related to unoptimized nanofabrication process and RF measurement design."

[28] M. Baumgartner *et al.*, "Spatially and time-resolved magnetization dynamics driven by spin–orbit torques," *Nat. Nanotechnol.*, vol. advance online publication, Aug. 2017.

[29] K.-S. Lee, S.-W. Lee, B.-C. Min, and K.-J. Lee, "Thermally activated switching of perpendicular magnet by spin-orbit spin torque," *Appl. Phys. Lett.*, vol. 104, no. 7, p. 072413, Feb. 2014.

[30] E. B. Myers, F. J. Albert, J. C. Sankey, E. Bonet, R. A. Buhrman, and D. C. Ralph, "Thermally Activated Magnetic Reversal Induced by a Spin-Polarized Current," *Phys. Rev. Lett.*, vol. 89, no. 19, p. 196801, Oct. 2002.

[31] J. Z. Sun, "Spin-current interaction with a monodomain magnetic body: A model study," *Phys. Rev. B*, vol. 62, no. 1, pp. 570–578, Jul. 2000.

[32] P. M. Braganca, O. Ozatay, A. G. F. Garcia, O. J. Lee, D. C. Ralph, and R. A. Buhrman, "Enhancement in spin-torque efficiency by nonuniform spin current generated within a tapered nanopillar spin valve," *Phys. Rev. B*, vol. 77, no. 14, p. 144423, Apr. 2008.

[33] J. Park, G. E. Rowlands, O. J. Lee, D. C. Ralph, and R. A. Buhrman, "Macrospin modeling of sub-ns pulse switching of perpendicularly magnetized free layer via spin-orbit torques for cryogenic memory applications," *Appl. Phys. Lett.*, vol. 105, no. 10, p. 102404, Sep.

2014.

[34] G. Yu *et al.*, "Magnetization switching through spin-Hall-effect-induced chiral domain wall propagation," *Phys. Rev. B*, vol. 89, no. 10, p. 104421, Mar. 2014.

[35] M. M. Decker *et al.*, "Time Resolved Measurements of the Switching Trajectory of Pt/Co Elements Induced by Spin-Orbit Torques," *Phys. Rev. Lett.*, vol. 118, no. 25, p. 257201, Jun. 2017.

[36] D. P. Bernstein *et al.*, "Nonuniform switching of the perpendicular magnetization in a spin-torque-driven magnetic nanopillar," *Phys. Rev. B*, vol. 83, no. 18, p. 180410, mai 2011.

[37] C. Zhang, S. Fukami, H. Sato, F. Matsukura, and H. Ohno, "Spin-orbit torque induced magnetization switching in nano-scale Ta/CoFeB/MgO," *Appl. Phys. Lett.*, vol. 107, no. 1, p. 012401, Jul. 2015.

[38] H. Sato *et al.*, "Junction size effect on switching current and thermal stability in CoFeB/MgO perpendicular magnetic tunnel junctions," *Appl. Phys. Lett.*, vol. 99, no. 4, p. 042501, Jul. 2011.

[39] J. Z. Sun *et al.*, "Effect of subvolume excitation and spin-torque efficiency on magnetic switching," *Phys. Rev. B*, vol. 84, no. 6, p. 064413, Aug. 2011.

[40] C. J. Durrant, R. J. Hicken, Q. Hao, and G. Xiao, "Scanning Kerr microscopy study of current-induced switching in Ta/CoFeB/MgO films with perpendicular magnetic anisotropy," *Phys. Rev. B*, vol. 93, no. 1, p. 014414, Jan. 2016.

[41] O. J. Lee *et al.*, "Central role of domain wall depinning for perpendicular magnetization switching driven by spin torque from the spin Hall effect," *Phys. Rev. B*, vol. 89, no. 2, p. 024418, Jan. 2014.

[42] D. Saida *et al.*, "Low-Current High-Speed Spin-Transfer Switching in a Perpendicular Magnetic Tunnel Junction for Cache Memory in Mobile Processors," *IEEE Trans. Magn.*, vol. 50, no. 11, pp. 1–5, Nov. 2014.

[43] L. Thomas *et al.*, "Perpendicular spin transfer torque magnetic random access memories with high spin torque efficiency and thermal stability for embedded applications (invited)," *J. Appl. Phys.*, vol. 115, no. 17, p. 172615, May 2014.

Figure caption

Fig.1 (a) Sketch of the three-terminal MTJ. (b) Scanning electron microscopy image of a 275 nm diameter MTJ on top of a 635 nm wide Ta track. (c) Resistance as a function of the magnetic field applied perpendicularly to the sample plane.

Fig. 2 (a) TMR as a function of the current pulse amplitude I_P (τ_P=0.55 ns long) in the presence of an external in-plane magnetic field $\mu_0 H_{ip}$=100 mT. The TMR is measured after the injection of the current pulse. The arrows show the sweep direction of I_P. (b) Switching probability (P_{sw}) from the P to the AP configuration as a function of I_P for three different pulse lengths τ_P=0.55 ns (black, square), τ_P=0.89 ns (red, circles) and τ_P=1 ns (blue, circles) at an applied field $\mu_0 H_{ip}$=100 mT.

Fig.3 (a) Switching current I_c as a function of the current pulse length τ_P for two values of the external in-plane magnetic field (P to AP switching). Inset: I_c vs $1/\tau_P$ for $\mu_0 H_{ip}$ = 100 mT. (b) Energy dissipated in a 3 kΩ resistor (simulating the resistance of the Ta track and the transistor) as a function of τ_P for two values of H_{IP} using the write current for the three-terminal device with a 635 nm wide Ta track. The blue scale on the right shows the write energy extrapolated for a 50 nm wide and 3 nm thick Ta track.
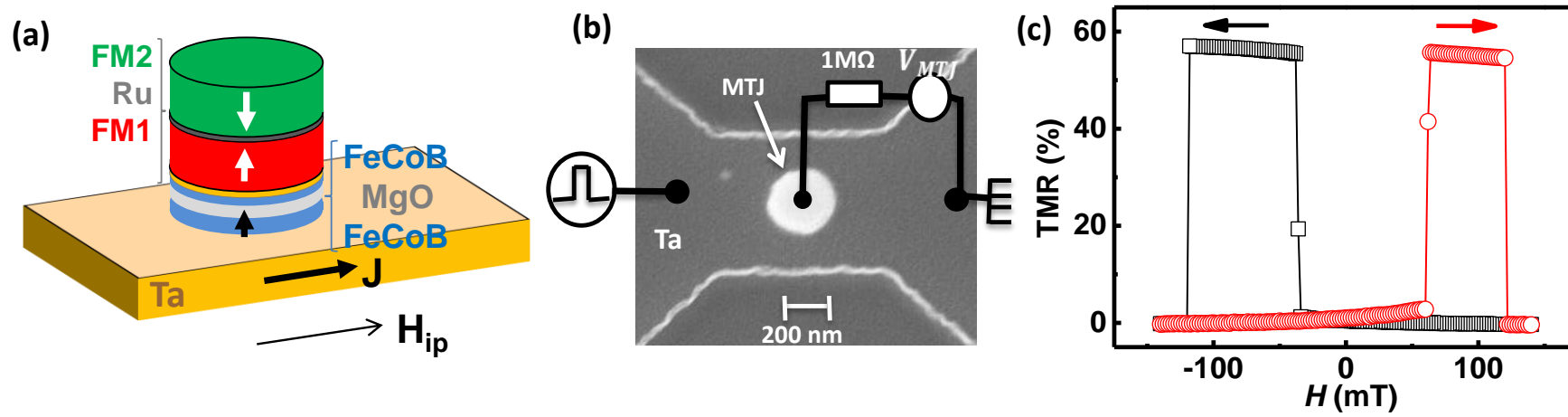
12

(a) FM2 Ru FM1 FeCoB MgO FeCoB Ta **J** H_{ip}
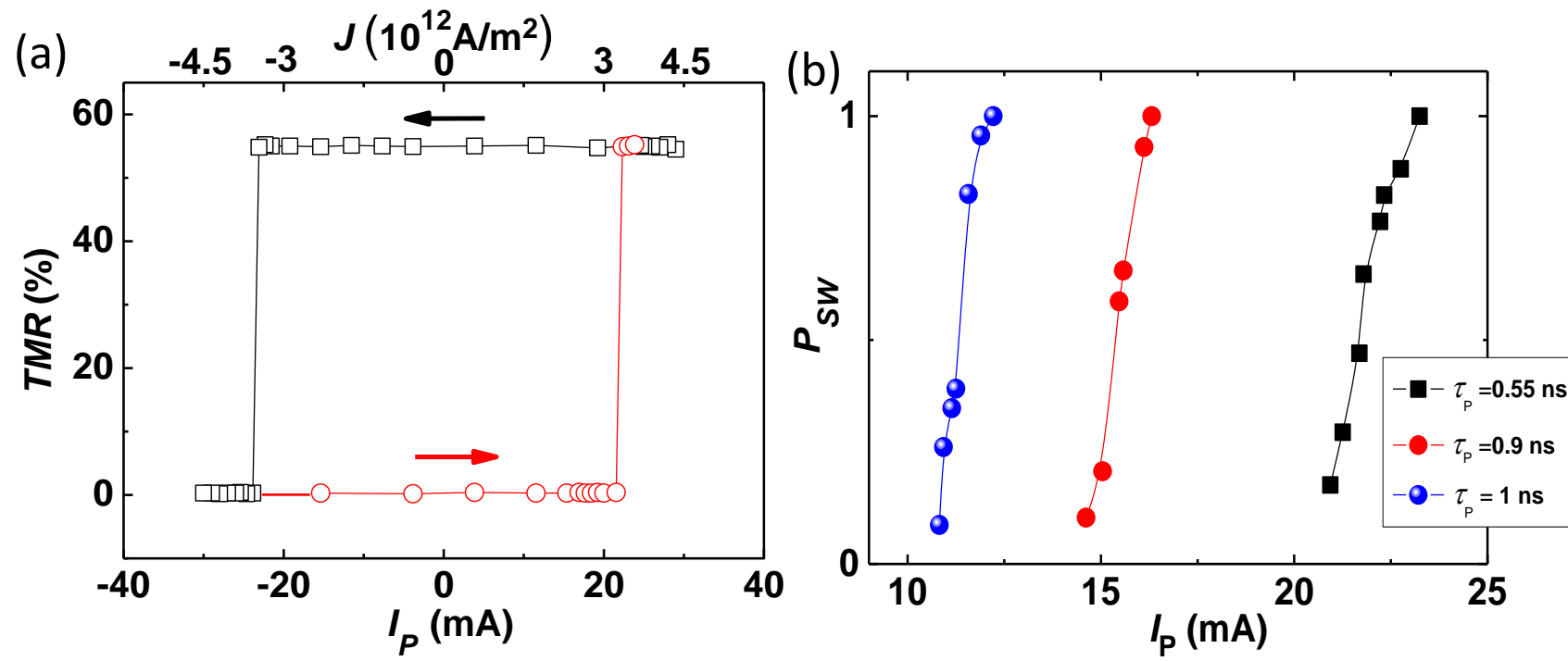
(b) MTJ 1MΩ V_{MTJ} Ta 200 nm

(c)

Fig. 1 Cubukcu *et al.*

13

Fig. 2. Cubukcu *et al*

Fig. 3. Cubukcu *et al.*